Time-Frequency Filtering Based on Model Fitting in the Time-Frequency Plane

Article *in* Signal Processing Letters, IEEE · March 2019

DOI: 10.1109/LSP.2019.2904148

3 authors:

Marcelo A. Colominas
National University of Entre Rios
39 PUBLICATIONS **3,781** CITATIONS
SEE PROFILE

Sylvain Meignen
University Joseph Fourier - Grenoble 1
99 PUBLICATIONS **3,468** CITATIONS
SEE PROFILE

Duong Hung Pham
Institut de Recherche en Informatique de Toulouse
38 PUBLICATIONS **788** CITATIONS
SEE PROFILE

Time-Frequency Filtering Based on Model Fitting in the Time-Frequency Plane

Marcelo A. Colominas, Sylvain Meignen, and Duong-Hung Pham

***Abstract*—The modulus of time-frequency representations, like the short-time Fourier or wavelet transforms, of a multicomponent signal exhibit ridges from which one usually computes estimations of the instantaneous frequencies of the modes making up the signal. But, due to the finite frequency resolution, the estimations thus obtained are piecewise constant. Our aim in this letter is to introduce a novel method for the estimation of the instantaneous frequencies of the modes based on the modeling of the modulus of the short-time Fourier transform, and then to propose a novel technique for mode retrieval. Numerical experiments carried out on both simulated and real signals demonstrate the benefits of the proposed approach over others based on the short-time Fourier transform.**

***Index Terms*—Time-frequency representation, instantaneous frequency, ridge extraction, mode retrieval.**

I. Introduction

VARIATIONS in frequencies of non-stationary signals have been a subject of study for the last 50 years. The characterization of such variations via *instantaneous frequency* (IF) can indeed be commonly encountered in various tasks e.g., pathology diagnosis [1]–[3], or structural damage [4], [5]. When studying multicomponent signals (MCSs) a common approach to compute the instantaneous frequencies (IFs) of the modes (or components) composing the signal is to compute its linear time-frequency (TF) representation, e.g. the short-time Fourier transform (STFT) or the continuous wavelet transform (CWT), and then look for *ridges* in the TF plane which are proved to be associated with the IFs of the components. Subsequently, the retrieval of a component is performed by inverting the TF representation in the vicinity of the corresponding ridge [6]. However, to proceed this way does not provide with accurate estimations of the IFs of the modes since the latter are based on the frequencies computed on the ridge and therefore belong to a *discrete* set of predefined frequencies. This is a consequence of the frequency binning when computing the STFT and the estimated IFs are piecewise constant functions, also making the computation of their derivatives called *chirp rates* (CRs) particularly difficult in that framework [7].

In this letter, we propose a new approach to the estimation of the IFs of the modes of MCSs using only the STFT modulus, which then enables straightforward mode retrieval. To that end, after having introduced some useful definitions in Section II, we recall in Section III a widely used procedure for IFs estimation and mode reconstruction based on the analysis of the ridges of the modulus of STFT and then explain why the discrete-time implementation limits the frequency resolution of these IFs estimations. Then, we present, in Section IV, our new method for the estimation of the IFs of the modes based on a *model fitting* (MF) derived from a local linear chirp approximation, and then show how to derive from this new technique a simple mode reconstruction procedure. Finally, numerical experiments carried out on artificial and real signals in Section V demonstrate the benefits brought by the proposed method, over existing ones based on STFT.

II. Multicomponent Signals and STFT

In what follows, we make an extensive use of a deterministic model of the so-called *multicomponent signal* (MCS) consisting of a superposition of a small number of components modulated in both amplitude and frequency (AM-FM). It is considered as a versatile way to model numerous phenomena e.g., audio signals [8], biomedical signals [9], or economic temporal series [10]. A signal made of L components can be written as:

$$x(t) = \sum_{l=1}^{L} x_l(t) = \sum_{l=1}^{L} A_l(t)\, e^{i2\pi\phi_l(t)}, \tag{1}$$

with $A_l(t), \phi_l'(t) > 0\,\forall t$, and $\phi_{l+1}'(t) > \phi_l'(t)\,\forall l$. Note that this model assumes the temporal variations of $A_l(t)$ to be small. The *analysis* of such signals in particular involves the estimation of the instantaneous amplitudes $A_l(t)$ and frequencies $\phi_l'(t)$, and/or the extraction of the *modes* $x_l(t)$.

To perform the analysis of such signals in the TF plane one often uses the (modified) Short Time Fourier Transform (STFT) defined by [11]

$$F_x^g(t,f) = \int_{-\infty}^{+\infty} x(u) g(u-t) e^{-i2\pi f(u-t)}\, du, \tag{2}$$

where $g(t)$ is an even real compactly supported window in the Fourier domain, i.e. $\mathrm{supp}\{\hat{g}(f)\} \subseteq [-B, +B]$.[1,2] The signals

Manuscript received December 30, 2018; revised March 6, 2019; accepted March 6, 2019. Date of publication March 11, 2019; date of current version March 22, 2019. The work of M. A. Colominas was supported by Project FP7 DESIRE (Health-F2-602531-2013). The work of D.-H. Pham was supported by the FRM under Grant DPP20151033957. The associate editor coordinating the review of this manuscript and approving it for publication was Dr. David I. Shuman. *(Corresponding author: Marcelo A. Colominas.)*

M. A. Colominas is with the LARIS-Laboratoire Angevin de Recherche en Ingénierie des Systèmes, University of Angers, 49000 Angers, France (e-mail: marcelo.colominas@univ-angers.fr).

S. Meignen is with the Jean Kuntzmann Laboratory, University of Grenoble-Alpes and CNRS UMR 5224, 38041 Grenoble, France (e-mail: sylvain.meignen@univ-grenoble-alpes.fr).

D.-H. Pham is with the ICube Laboratory, Télécom Physique Strasbourg and CNRS UMR 7357, 67412 Illkirch, France (e-mail: dhpham@unistra.fr).

Digital Object Identifier 10.1109/LSP.2019.2904148

[1] This is only an approximation since the compact-supportness of g prevents $\hat{g}$ from having a compact support.

[2] $\hat{g}(f) = \int g(t) e^{-i2\pi f t}\, dt$ is the Fourier transform (FT) of $g(t)$.

modeled as in (1) have a particular structure in the TF plane: every component occupies a "ribbon" around its IF $\phi_l'(t)$ [12]. If the $\phi_l'(t)$ s are well separated (i.e. $\phi_{l+1}'(t) - \phi_l'(t) > 2B$), then each component "lives" in non-overlapping domains [13], [14].

III. STFT-Based Mode Extraction

A usual strategy for the retrieval the modes of an MCS based on STFT is to estimate the IFs arising from the above mentioned structure of the STFT. In order to find the dominant lines, called *ridges*, the following non-convex optimization problem should be solved [13]:

$$\max_{\mathcal{C}} \sum_{l=1}^{L} \int_{-\infty}^{+\infty} (|F_x^g(t, c_l(t))|^2 - \alpha c_l'(t)^2 - \beta c_l''(t)^2) dt, \quad (3)$$

where $\mathcal{C} = \{c_1(t), c_2(t), \ldots, c_L(t)\}$ is the set of ridges and α and β are regularization parameters favoring the continuity and smoothness of the solutions, respectively.

Once the ridges are estimated, the l-th mode can be reconstructed by integrating the STFT in the vicinity of the corresponding ridge $c_l(t)$:

$$x_l(t) \approx \frac{1}{g(0)} \int_{c_l(t)-\eta_l^-(t)}^{c_l(t)+\eta_l^+(t)} F_x^g(t, f) df, \quad (4)$$

where the functions $\eta_l^-(t)$ and $\eta_l^+(t)$ are respectively the ribbon inferior and superior half-width which need to be estimated.

In the discrete-time setting, working with $x[n]$, the STFT becomes:

$$F_x^g[n, k] = \sum_u x[u] g[u-n] e^{-i2\pi k \Delta f (u-n)}, \quad (5)$$

with $k \in \mathbb{N}$ and Δf the frequency resolution. For finite time series of length N, the time index n ranges from 1 to N, and the frequency index k from 0 to $K-1$, with $K\Delta f = 1$ (the maximum possible normalized frequency).

In that framework, problem (3) leads to:

$$\max_{\mathcal{C}} \sum_{l=1}^{L} \sum_{n=1}^{N} |F_x^g[n, c_l[n]]|^2 - \alpha(\Delta^1 c_l[n])^2 - \beta(\Delta^2 c_l[n])^2, \quad (6)$$

where $\mathcal{C} := (c_l)_{l=1,\ldots,L}$, with ':=' meaning definition, $c_l : \{1, \ldots, N\} \mapsto \{0, \ldots, K-1\}$, $\Delta^1 c_l[n] = c_l[n+1] - c_l[n]$ and $\Delta^2 c_l[n] = c_l[n+1] - 2c_l[n] + c_l[n-1]$ replacing $c_l'(t)$ and $c_l''(t)$ in (3), respectively. In this case, a given ridge $c_l[n]$ is constrained by the frequency binning limiting the resolution of the obtained IFs and leading to piecewise constant IFs approximations [7]. In practice, the ridges are extracted one by one starting from a random time and the final result is obtained by averaging over different initial times [7], [15]. The reconstruction of x_l is then performed through:

$$x_l[n] \approx \frac{1}{g(0)K} \sum_{c_l[n]-\eta_l^-[n]}^{c_l[n]+\eta_l^+[n]} F_x^g[n, k]. \quad (7)$$

Note that in the discrete-time context, η_l^- and η_l^+ are integers. To estimate these parameters in a noisy scenario, a hard-thresholding (HT) strategy might be adopted [16], [17] using robust estimates of the variance of the STFT of the noise [18].

IV. Instantaneous Frequency Estimation and Mode Reconstruction Based on Model Fitting

A. Local Linear Chirp Approximation

Let us consider the linear chirp $x(t) = e^{i2\pi(at+bt^2)}$. Its STFT reads [14]:

$$\begin{aligned} F_x^g(t, f) &= x(t) \int_{-\infty}^{+\infty} g(u) e^{i2\pi b u^2} e^{-i2\pi(f-(a+2bt))u} du \\ &= x(t) \widehat{g_{\phi''}}(f - \phi'(t)), \end{aligned} \quad (8)$$

with $g_{\phi''}(t) = g(t) e^{i2\pi \frac{\phi''}{2} t^2}$, $\phi'(t)$ being the IF of x and $\phi''(t) = 2b$ its instantaneous CR. When using the Gaussian window $g(t) = e^{-\sigma t^2}$, $\sigma > 0$, Eq. (8) can be rewritten as [19]:

$$F_x^g(t, f) = x(t) \sqrt{\frac{\pi}{\sigma - i\pi\phi''}} e^{\frac{-\sigma\pi^2(f-\phi'(t))^2}{\sigma^2+\pi^2\phi''^2}} e^{\frac{-i\phi''\pi^3(f-\phi'(t))^2}{\sigma^2+\pi^2\phi''^2}}. \quad (9)$$

We can then think of more complicated signals $x(t) = A(t)e^{i2\pi\phi(t)}$, which, however, admits *locally* a linear chirp approximation:

$$x(u) \approx x(t) e^{i2\pi(\phi'(t)(u-t) + \frac{\phi''(t)}{2}(u-t)^2)}, \quad (10)$$

for u sufficiently close to t. This approximation is all the better that the third derivative of the phase function is small. Eq. (10) allows us to approximate the STFT at each time instant t using Eq. (9), except this time ϕ'' is a function of t.

B. New IF Estimation Based on STFT Modulus Approximation

As highlighted above, the mode reconstruction strategy based on STFT consists of the estimation of the "ribbons" occupied by the modes in the TF plane. Staying in line with this, from Eq. (9), we define, for every t, a model with two free parameters:

$$\rho(f, \tilde{\phi}'(t), \tilde{\phi}''(t)) = \sqrt{\frac{\pi}{\sqrt{\sigma^2 + \pi^2\tilde{\phi}''(t)^2}}} e^{\frac{-\sigma\pi^2(f-\tilde{\phi}'(t))^2}{\sigma^2+\pi^2\tilde{\phi}''(t)^2}}, \quad (11)$$

and estimate the IFs of a given MCS by solving the following problem:

$$\max_{\Phi} \sum_{l=1}^{L} \int_{-\infty}^{+\infty} \int_{-\infty}^{+\infty} |F_x^g(t, f)| \rho(f, \tilde{\phi}_l'(t), \tilde{\phi}_l''(t)) df\, dt, \quad (12)$$

where $\Phi := (\tilde{\phi}_l', \tilde{\phi}_l'')_{l=1,\ldots,L}$ are the IFs and absolute values of the CRs, respectively. This is nothing more than problem (3) in which the square modulus of the STFT is replaced by the modulus and the Dirac function in the first term $|F_x^g(t, c(t))|^2 = \int |F_x^g(t, f)|^2 \delta(f - c(t)) df$ by the function ρ.[3] Note also that in (12), we set the regularization parameters α and β to zero since these are not very relevant for ridge extraction according to an analysis carried out in [7].[4] Therefore, instead of looking for the maximum of the spectrogram at each t, we compute the maximum of the *inner product* in L^2, with respect to

[3] One must bear in mind that $\int |F_x^g(t, f)| \rho(f, \tilde{\phi}'(t), \tilde{\phi}''(t)) df$ in Eq. (12) is a function of t.

[4] For the multicomponent case, given a local maximum at time t, at neighboring times we look for maxima of the cost function in an interval related to time t, corresponding to setting an upper bound on ϕ''.

variable f, of the modulus of the STFT with the function ρ. To be more specific, it can be easily proven that if $x(t) = e^{i2\pi(at+bt^2)}$, then $\nabla_{\tilde{\phi}',\tilde{\phi}''}\langle|F_x^g(t,f)|, \rho(f,\tilde{\phi}'(t),\tilde{\phi}''(t))\rangle = 0$, for a given t, if and only if $\tilde{\phi}'(t) = \phi'(t) = a + 2bt$ and $\tilde{\phi}''(t) = \phi''(t) = 2b$, where ∇ and $\langle .,. \rangle$ denote respectively the *gradient* and *inner product* operators. This means that problem (12) has a unique optimum, which can be found thanks to optimization methods without derivatives, e.g. the golden-section search [20], in which each variable is independently treated. More precisely, the search is carried out in two steps: first one seeks the optimum IF, and then the optimum absolute value of CR. Such a strategy is possible as a result of $\frac{\partial}{\partial\tilde{\phi}'}\langle|F_x^g(t,f)|, \rho(f,\tilde{\phi}',\tilde{\phi}'')\rangle|_{\tilde{\phi}'=a+2bt} = 0$ regardless the value of $\tilde{\phi}''$. This means that the problem, when seen as a function of only $\tilde{\phi}'$, also has a unique maximum. So, one can set $\tilde{\phi}'' = 0$ as a first step, optimize on $\tilde{\phi}'$ and then on $\tilde{\phi}''$. It is also worthy of note that the golden-section search does not need to compute derivatives and works in the studied discrete-time framework. However in noisy situations, the problem is no longer unimodal although the optimum for IF is robust. In this regard, we propose to apply a pre-step consisting of hard-thresholding (HT) the initial STFT before solving the optimization problem [17], [18]. For a more general multicomponent case, a peeling scheme is adopted, extracting one mode at a time, and continuing with the difference between the input STFT and the resultant one.

In a discrete-time framework, one can transpose the above analysis to that of a discrete-time signal $x[n] = e^{i2\pi(an+bn^2)}$ as:

$$F_x^g[n,k] \approx x[n]\sqrt{\frac{\pi}{\sigma - i\pi\phi''}}e^{\frac{-\sigma\pi^2(k\Delta f-\phi'[n])^2}{\sigma^2+\pi^2\phi''^2}}e^{\frac{-i\phi''\pi^3(k\Delta f-\phi'[n])^2}{\sigma^2+\pi^2\phi''^2}}, \tag{13}$$

where $\phi'[n] = a + 2bn$ is the real-valued IF of $x[n]$ and $\phi'' = 2b$ its CR. Then, a discrete-time version of (12) is implemented:

$$\max_{\Phi}\sum_{l=1}^{L}\sum_{n=1}^{N}\sum_{k=0}^{K-1}|F_x^g[n,k]|\rho(k\Delta f,\tilde{\phi}_l'[n],\tilde{\phi}_l''[n]), \tag{14}$$

where

$$\rho(k\Delta f,\tilde{\phi}_l'[n],\tilde{\phi}_l''[n]) = \sqrt{\frac{\pi}{\sqrt{\sigma^2+\pi^2\tilde{\phi}''[n]^2}}}e^{\frac{-\sigma\pi^2(k\Delta f-\tilde{\phi}'[n])^2}{\sigma^2+\pi^2\tilde{\phi}''[n]^2}}, \tag{15}$$

is the discretization of (11). The set $\Phi := (\tilde{\phi}_l', \tilde{\phi}_l'')_{l=1,\ldots,L}$ is composed of mappings $\tilde{\phi}_l', \tilde{\phi}_l'' : \{1,\ldots,N\} \mapsto \mathbb{R}$. It is worth recalling that in the traditional ridge estimation, the obtained ridges are mappings from $\{1,\ldots,N\}$ to $\{0,\ldots,K-1\}$, giving birth to piecewise constant IFs, called staircase effect [7]. On the contrary, Eq. (14) offers the possibility to estimate the IFs as real-valued functions.

The computational cost of our proposal is higher than that of traditional ridge estimation. While in ridge estimation (Eq. (3)) there is only one optimization, our proposal involves two: one for IF, and one for CR. The computational cost can be controlled by the maximum number of iterations allowed for the golden-section search algorithm [20].

Algorithm 1: Model Fitting (MF) on STFT.

1: **Input:** $F_x^g[n,k]$, σ, Δf
2: Compute HT $\overline{F_x^g}[n,k]$ of $F_x^g[n,k]$ [17], [18]
3: Define $\rho(k\Delta f,\tilde{\phi}_l',\tilde{\phi}_l'')$ according to Eq. (11)
4: **for** $n = 1, 2, \ldots,$N **do**
5: Set $\tilde{\phi}_l'[n] = 0$ and $\tilde{\phi}_l''[n] = 0$
6: Optimize Eq. (14) on $|\overline{F_x^g}[n,k]|$ for $\tilde{\phi}_l'$
7: With the obtained $\hat{\tilde{\phi}}_l'$, optimize for $\tilde{\phi}_l''$
8: $|F_{x_l}^g[n,k]_{est}| := \frac{\langle|\overline{F_x^g}[n,k]|,\rho(k\Delta f,\hat{\tilde{\phi}}_l',\hat{\tilde{\phi}}_l''))\rangle}{\|\rho(k\Delta f,\hat{\tilde{\phi}}_l',\hat{\tilde{\phi}}_l'')\|_2^2}\rho(k\Delta f,\hat{\tilde{\phi}}_l',\hat{\tilde{\phi}}_l'')$
9: **end for**
10: Define $F_{x_l}^g[n,k]_{est} = |F_{x_l}^g[n,k]_{est}|e^{i\arg F_x^g[n,k]}$
11: **Output:** $F_{x_l}^g[n,k]_{est}$, $\tilde{\phi}_l'[n]$, $\tilde{\phi}_l''[n]$

C. Mode Reconstruction

Once the IF and the absolute value of the CR are computed, the modulus of the STFT can be estimated by:

$$|F_x^g[n,k]_{est}| = \frac{\langle|F_x^g[n,k]|,\rho(k\Delta f,\hat{\tilde{\phi}}'[n],\hat{\tilde{\phi}}''[n])\rangle}{\|\rho(k\Delta f,\hat{\tilde{\phi}}'[n],\hat{\tilde{\phi}}''[n])\|_2^2}\rho(k\Delta f,\hat{\tilde{\phi}}'[n],\hat{\tilde{\phi}}''[n]), \tag{16}$$

where $\hat{\tilde{\phi}}'$ and $\hat{\tilde{\phi}}''$ are the solutions of (14), and $\|.\|_2$ is the ℓ_2 norm. Note that $\langle|F_x^g[n,k]|,\rho(k\Delta f,\hat{\tilde{\phi}}',\hat{\tilde{\phi}}'')\rangle/\|\rho(k\Delta f,\hat{\tilde{\phi}}',\hat{\tilde{\phi}}'')\|_2^2$ constitutes an estimation of $|x[n]|$. Finally, the STFT of the mode is approximated by

$$F_{x_l}^g[n,k]_{est} = \left|F_{x_l}^g[n,k]_{est}\right| e^{i\arg F_x^g[n,k]}, \tag{17}$$

where the argument (phase) of the original STFT is used. Finally, one gets the reconstructed mode by inverting the STFT using Eq. (7). The whole procedure is detailed in the Algorithm 1 that we coin MF in the sequel.

V. Results and Discussion

This section presents some numerical results on artificial and real signals to illustrate the interest of MF over existing methods based on STFT for IF estimation and mode retrieval. To do so, we consider synthesized signals of length $N = 1000$, whose STFTs are computed with K frequency bins ($\Delta f = 1/K$) and with a Gaussian window whose length parameter σ is determined by means of Rényi entropy technique [21]. Also, the signals are contaminated by white Gaussian noises leading to different *Signal-to-Noise Ratios* (SNRs). The performance of the IF estimation and mode reconstruction are evaluated by $SNR_{out}(\prod) = 20\log_{10}\left(\|\prod_{ref}\|/(\|\prod_{ref} - \prod\|)\right)$, with $\|.\|$ being the ℓ_2 norm for IF estimation and the Frobenius norm for STFT estimation. Note that the latter is used to evaluate the performance of mode reconstruction, because in the tested methods once an approximation of the STFT is found the same reconstruction algorithm is applied. The first row of Fig. 1 depicts the modulus of the STFTs with $K = 0.1N$ for the three following signals:

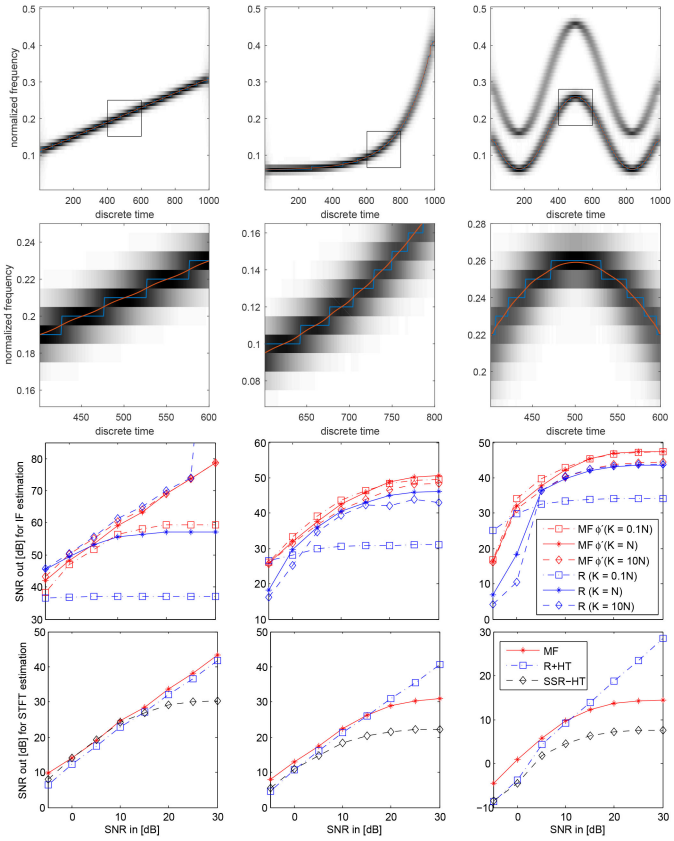

Fig. 1. First row, three different types of MCS, with a zoom on the STFT on which the ridges and the IF estimted via MF are superimposed. Third row: Performance in IF and STFT estimation. *Left*: linear chirp. *Middle*: exponential chirp. *Right*: two-component signal. MF: Model Fitting on STFT (the proposed algorithm). MF ϕ': estimated IF using MF. R: ridge extracted by the technique introduced in [7]. SSR-HT: Shifted-Symmetrized-Regularized Hard-Thresholding [17]. R+HT: ridge extraction followed by HT [17].

Linear chirp. $x[n] = \exp(i(2\pi \times 10^{-1} n + 2\pi \times 10^{-1} n^2))$, with $\phi'_{ref}[n] = 10^{-1} + 2 \times 10^{-4} n$ and $\phi''_{ref} = 2 \times 10^{-4}$.

Exponential chirp. $x[n] = \exp(i(2\pi 5 \times 10^{-2} n + e^{6\times 10^{-3} n}))$, with $\phi'_{ref}[n] = 5 \times 10^{-2} + 6e^{6\times 10^{-3} n}/(2\pi)$ and $\phi''_{ref}[n] = 36e^{6\times 10^{-3} n}/(2\pi)$.

Sinusoidal chirp. $x[n] = \exp(i(2\pi 1.5 \times 10^{-1} n + 2/3 \times 10^{-1} \cos(3\pi \times 10^{-3} n)))$, with $\phi'_{ref}[n] = 1.5 \times 10^{-1} - 10^{-1} \sin(3\pi \times 10^{-3} n)$ and $\phi''_{ref}[n] = -3\pi \times 10^{-1} \cos(3\pi \times 10^{-3} n)$.

The second row of Fig. 1 displays a zoom of the STFT modulus along with the ridges extracted using the technique carried out in [7] and the IF estimation obtained via MF. It can be seen that the staircase effect is completely eliminated by the latter. In the third row, we show the stability of the IF estimation of the studied techniques in terms of SNR_{out} with respect to different frequency resolutions K.

Observation shows that while the MF algorithm gives similar results for all values of K, the method in [7] suffers from the frequency resolution problem. A possibility to reduce the staircase effect is zero-padding [7], but then much more data needs to be stored.

The results of the stability of the STFT estimation using $K = N$ are displayed in the fourth row of of Fig. 1. It is obvious

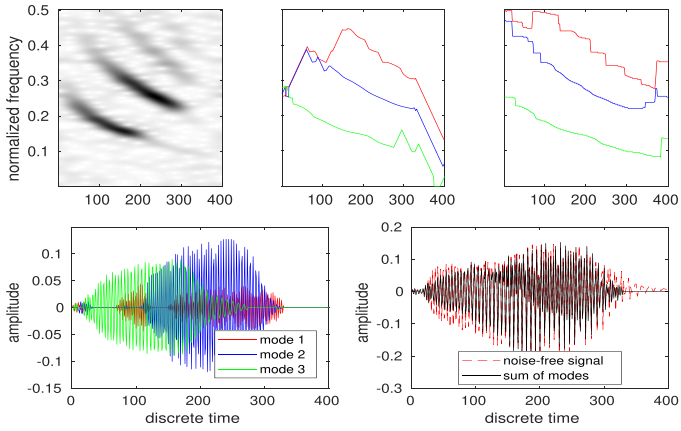

Fig. 2. Bat signal. First row: noisy STFT modulus, IFs computed by MF and those obtained by the technique introduced in [7]. Second row: the three reconstructed modes obtained by MF and the reconstructed signal along with the original noise-free one.

that MF is superior for linear chirps, and for the other types of signal for low SNRs. As the input SNR increases, the R+HT method achieves the best results since the signal is farther from our local linear chirp model.

Bat echolocation. The example on a real signal corresponds to a bat echolocation signal,[5] polluted by a white Gaussian noise such that the input SNR is 5.0 dB. The STFT modulus of the noisy signal is shown in the first row of Fig. 2, together with the IFs estimated by MF algorithm and the ones computed by the technique in [7]. The staircase effect is clearly removed using the former, which however faces some difficulties in estimating the IF of the high frequency mode. The difficulties are mainly present in those times where the amplitudes of the modes are very small, which is known to be a problem for IF estimation. Finally, a comparison between the reconstructed signal and the original noise-free one results in an output SNR of 9.78 dB, which confirms the applicability of MF to real signals. For the same signal, SSR-HT achieved an output SNR of 8.79 dB.

VI. Conclusions

In this letter, we have proposed a novel approach for the TF filtering and IF estimation based on model fitting in the TF plane. The main expected advantages are: (1) smoother STFTs, as opposed to the ones obtained via ridge extraction and hard-thresholding, which leads to the better mode estimation; (2) smoother IFs estimates than those based on ridge extraction; (3) a direct estimation of the absolute value of the instantaneous CR as opposed to those obtained via finite differences of the modulus of STFT on the ridge. We have presented here only the main ideas of the model fitting approach along with some supporting examples, but further studies should naturally be performed to assess even better the optimum parameters and in particular the chirp rate.

[5]Thanks to A. Feng of the University of Illinois for the bat signal and the permission to use it in this work.

REFERENCES

[1] S. Cerutti, A. L. Goldberger, and Y. Yamamoto, "Recent advances in heart rate variability signal processing and interpretation," *IEEE Trans. Biomed. Eng.*, vol. 53, no. 1, pp. 1–3, Jan. 2006.

[2] U. R. Acharya, K. P. Joseph, N. Kannathal, L. C. Min, and J. S. Suri, "Heart rate variability," in *Advances in Cardiac Signal Processing*, Berlin, Germany: Springer, 2007, pp. 121–165.

[3] M. Malik and A. J. Camm, *Dynamic Electrocardiography*. Hoboken, NJ, USA: Wiley, 2008.

[4] O. Salawu, "Detection of structural damage through changes in frequency: A review," *Eng. Struct.*, vol. 19, no. 9, pp. 718–723, 1997.

[5] C. R. Farrar, S. W. Doebling, and D. A. Nix, "Vibration-based structural damage identification," *Philos. Trans. Roy. Soc. London A, Math., Phys., Eng. Sci.*, vol. 359, no. 1778, pp. 131–149, 2001.

[6] F. Auger *et al.*, "Time-frequency reassignment and synchrosqueezing: An overview," *IEEE Signal Process. Mag.*, vol. 30, no. 6, pp. 32–41, Nov. 2013.

[7] S. Meignen, D.-H. Pham, and S. McLaughlin, "On demodulation, ridge detection, and synchrosqueezing for multicomponent signals," *IEEE Trans. Signal Process.*, vol. 65, no. 8, pp. 2093–2103, Apr. 2017.

[8] S. Mallat, *A Wavelet Tour of Signal Processing: The Sparse Way*. New York, NY, USA: Academic, 2009.

[9] H.-T. Wu, Y.-H. Chan, Y.-T. Lin, and Y.-H. Yeh, "Using synchrosqueezing transform to discover breathing dynamics from ECG signals," *Appl. Comput. Harmon. Anal.*, vol. 36, no. 2, pp. 354–359, 2014.

[10] X. Zhang, K. K. Lai, and S.-Y. Wang, "A new approach for crude oil price analysis based on empirical mode decomposition," *Energy Econ.*, vol. 30, no. 3, pp. 905–918, 2008.

[11] L. Cohen, *Time-Frequency Analysis*, vol. 1. Englewood Cliffs, NJ, USA: Prentice-Hall, 1995.

[12] R. Carmona, W. L. Hwang, and B. Torrésani, "Multiridge detection and time-frequency reconstruction," *IEEE Trans. Signal Process.*, vol. 47, no. 2, pp. 480–492, Feb. 1999.

[13] R. Carmona, W. L. Hwang, and B. Torrésani, "Characterization of signals by the ridges of their wavelet transforms," *IEEE Trans. Signal Process.*, vol. 45, no. 10, pp. 2586–2590, Oct. 1997.

[14] T. Oberlin, S. Meignen, and V. Perrier, "Second-order synchrosqueezing transform or invertible reassignment? Towards ideal time-frequency representations," *IEEE Trans. Signal Process.*, vol. 63, no. 5, pp. 1335–1344, Mar. 2015.

[15] G. Thakur, E. Brevdo, N. S. Fučkar, and H.-T. Wu, "The synchrosqueezing algorithm for time-varying spectral analysis: Robustness properties and new paleoclimate applications," *Signal Process.*, vol. 93, no. 5, pp. 1079–1094, 2013.

[16] S. Meignen and D. H. Pham, "Retrieval of the modes of multicomponent signals from downsampled short-time fourier transform," *IEEE Trans. Signal Process.*, vol. 66, no. 23, pp. 6204–6215, Dec. 2018.

[17] D.-H. Pham and S. Meignen, "A novel thresholding technique for the denoising of multicomponent signals," in *Proc. IEEE Int. Conf. Acoust., Speech, Signal Process.*, 2018, pp. 4004–4008.

[18] D. L. Donoho and J. M. Johnstone, "Ideal spatial adaptation by wavelet shrinkage," *Biometrika*, vol. 81, no. 3, pp. 425–455, 1994.

[19] T. Oberlin, S. Meignen, and S. McLaughlin, "A novel time-frequency technique for multicomponent signal denoising," in *Proc. 21st Eur. Signal Process. Conf.*, 2013, pp. 1–5.

[20] R. P. Brent, *Algorithms for Minimization Without Derivatives*. North Chelmsford, MA, USA: Courier Corporation, 2013.

[21] R. G. Baraniuk, P. Flandrin, A. J. Janssen, and O. J. Michel, "Measuring time-frequency information content using the Rényi entropies," *IEEE Trans. Inf. Theory*, vol. 47, no. 4, pp. 1391–1409, May 2001.